



Transformation and Leaching Simulation of 6:2 and 8:2 diPAP and Related Metabolites in Unsaturated Soil Column Studies with MACRO

Eva Weidemann¹ · Matthias Gassmann¹

Received: 18 October 2022 / Accepted: 4 October 2023 / Published online: 14 October 2023
© The Author(s) 2023

Abstract

PFAS (perfluoroalkyl substances) are widespread in the environment and are found in almost every medium. Besides persistent PFAS, their transforming precursors gained attention since they may be a reservoir for persistent PFAS in soil. Only little information is available about the behavior of these precursors and the simultaneous leaching of their transformation products. However, this information is urgently needed to improve estimates of contamination levels. For this purpose, two precursors and their non-degradable metabolites were simulated using the MACRO model, with parameter values optimized using the evolutionary algorithm caRamel. A constant first-order transformation rate did not adequately represent the leaching of transformation products, but a variable transformation rate that decreased at the date of an equilibrium soil moisture provided a good representation of the precursor transformation and leaching of transformation products. The results are new evidence that variable environmental parameters such as soil moisture may affect the transformation rate of precursors. The simulation study is a step towards describing the behavior of PFAS precursors through physically-based models.

Keywords PFAS · diPAP · MACRO

1 Introduction

Perfluoroalkyl substances (PFAS) are anthropogenic pollutants, which are ubiquitous in the environment. The number of known PFAS is still uncertain but currently estimated to comprise 10,776 compounds [1]. The strong C-F-bond can lead to a persistent behavior [2], which is why the subgroup perfluoroalkyl acids (PFAA) is well-known. The tendency to persistence is the reason for the PFAS alias “forever chemicals.” Besides persistence, bioaccumulation potential, toxicity, carcinogenic and teratogenic effects are associated with some PFAS such as PFOA [3], which is why they should not be introduced into the environment. However, there are not only stable but also degradable PFAS, known as precursors. They can transform into persistent PFAA, making them at least as dangerous as their degradation products.

Polyfluoroalkyl phosphate diesters (diPAP) are precursors of the group of polyfluoroalkyl phosphate esters (PAP) and are known to biotransform into several intermediates [4]. The persistent final transformation products of diPAP, perfluorocarboxylic acids (PFCA) [4], are part of the PFAA group. diPAP are primarily used for their surfactant properties in the paper industry [5] and have been found in indoor air and dust [6], human sera [7], and agricultural soils [8]. Once present in soil, diPAP can pose a long-term problem due to their predicted low solubility [9] and high sorption potential, causing them to remain in the upper soil layers [10]. There, they transform into more mobile PFCA and other transformation products, which can be taken up by plants [11], leach through the vadose zone into the groundwater [12], or remain in the soil [13].

To test hypotheses and assess the environmental fate of chemicals in soil and groundwater, a variety of leaching models have been developed, including MACRO [14] and HYDRUS [15]. The selection of a suitable model depends on factors such as availability (open source or purchase), model type (physically driven, conceptual, empiric), temporal resolution and spatial resolution, and implemented processes. MACRO, for example, is used in pesticide

✉ Eva Weidemann
eva.weidemann@uni-kassel.de

¹ Department of Hydrology and Substance Balance,
University of Kassel, Kurt-Wolters-Str. 3, 34125 Kassel,
Germany

registration procedures [16] but is also used to simulate the leaching of other substances such as pharmaceuticals [17], nutrients [18], and veterinary antibiotics [19]. Simulation studies have also effectively described the behavior of PFAA in soils [20–22] using different approaches, including air–water-interface [21, 22], non-extractable residues [20], and different models [23].

Depending on the number of parameters and the complexity of the model, the calibration process of such models can be a challenge. Often, several parameter sets lead to comparably good results (equifinality [24]), or the used optimization algorithm is stuck in a local optimum [25]. For the determination of optima, algorithms are used which are aimed at minimizing or maximizing an objective function by automatic parameter variations. Especially in substance fate modeling, it can be necessary to optimize several objectives simultaneously, which does not simplify the problem solution process (multiobjective optimization). Optimization algorithms are categorized into local and global optimization [26]. Furthermore, global optimization algorithms can be divided into the categories evolutionary and deterministic [27]. Some optimization algorithms are implemented into R packages such as hydroPSO [28] and caRamel [29]. To the best of our knowledge, no previous simulation study has addressed the simultaneous transformation of precursors and leaching of their transformation products in soil. Therefore, this study describes the processes of leaching and transformation of 6:2 diPAP and 8:2 diPAP and their transformation products in a prior soil column study [10] using the physically based model MACRO. Both precursors were found in soil from an agricultural contaminated site in Germany among other PFAS [10]. Simulation results are not only used to disentangle underlying processes but may also help to estimate risks coming from contaminated soils.

2 Materials and Methods

2.1 Soil Column Study

The two-year soil column study, on which the simulations are based, was conducted between 2019 and 2021 (742 days). Detailed information about the experimental setup is available in [10]. Soil properties (Table S3), water input protocol (Table S4), masses in percolation water (Table S6–S8), and masses in soil at the end of study (Table S9–S11) can be found in the supplementary information (SI).

Different contamination strategies were realized within six variants. Here, three out of six variants are focused: (1) 6:2 diPAP, (2) 8:2 diPAP, and (3) PFCA. In this simulation study, only five out of ten applied PFAA of variant (3) are included, those which are transformation products (PFCA') of 6:2 and 8:2 diPAP. diPAP was mixed into sandy loam,

and PFAA were applied to the soil surface of sandy loam, which were both used as upper soil and dried at room temperature. diPAP was mixed into the soil three months before the study began and stored under dry and dark conditions. The lower half of the column was filled with a different sandy loam soil, which was PFAS-free and pre-wetted before adding the upper soil. The height of the soil was 50 cm, and the diameter of the columns 4.6 cm. The water input to the soil columns (35 ml/week) was done on three to five days a week, which ensured a uniform moisture level, but never full saturation, considering the soil as a whole. The consequential percolation was analyzed biweekly. The soil was analyzed before the study and in four different depths at the end. 6.1 mol-% diPAP and 1.0 mol-% PFCA' were still adsorbed to soil particles at the end of the 6:2 diPAP study. 41.9 mol-% PFCA' was found in the percolation water, and 51.0 mol-% was not recovered. In the 8:2 diPAP study, 44.7 mol-% untransformed 8:2 diPAP and 1.4 mol-% PFCA' were found in soil, 22.3 mol-% was found in the percolate, and 31.6 mol-% was not recovered. All mass balances were calculated, implying a transformation maximum of 200% regarding the initial mass of diPAP, since one mol diPAP can be transformed into 2 mol PFCA' [4]. The formation fraction ff of each PFCA was calculated by

$$ff = \frac{m_{PFCA'}}{m_{diPAP'}}, \quad (1)$$

with the PFCA' mass $m_{PFCA'}$ (μg) divided by the complete transformed mass of the respective precursor $m_{diPAP'}$ (6:2 diPAP': 497.5 μg ; 8:2 diPAP': 274.4 μg). During the transformation process, approximately 70% of transformed diPAP masses were transformed into metabolites (Table 1).

2.2 MACRO

MACRO is a numerical model that simulates one-dimensional water flow and solute transport [14]. It is

Table 1 Observations of PFCA transformation products (PFCA') in soil column systems at the end of diPAP studies. The formation fraction ff is calculated using the recovered transformed mass of 497.5 μg (6:2 diPAP') and 274.4 μg (8:2 diPAP')

PFCA'	6:2 diPAP		8:2 diPAP	
	Mass μg	ff –	Mass μg	ff –
PFBA'	25.1	0.05	2.9	0.01
PFPeA'	206.9	0.42	6.2	0.02
PFHxA'	111.7	0.22	8.6	0.03
PFHpA'	1.2	<0.01	28.5	0.10
PFOA'	–	–	170.4	0.62

commonly used for pesticide registration procedures [30] but has also been applied in a previous study on PFAS [20]. In this study, the command line version of MACRO 5.2 was used, managed via GNU R, and the results were analyzed using the macrouils package (1.15.0), as recommended by the MACRO developers [31]. The following descriptions of model features solely cover those which were found as the most relevant ones for the present modeling study. Further information can be taken from the technical description [14].

The model calculates evapotranspiration using either the Penman–Monteith equation and meteorological data or potential evapotranspiration and temperature. The model is divided into two domains, micropores and macropores, each with dual permeability. Water flow is determined using the Richards' equation for micropores and a gravity-driven equation for macropores. The solute flow is described by a convection–dispersion equation for micropores and a convection equation for macropores. The most relevant processes of the convection–dispersion equation for our simulation study are mass exchange between micro- and macropores, sorption, biodegradation, and solute leaching at the lower boundary. The adsorbed concentration of the solute in instantaneous equilibrium s is calculated using the Freundlich isotherm

$$s = K_D \cdot c^n, \quad (2)$$

which incorporates the sorption coefficient K_D (l/kg), the concentration of the solute in the liquid phase c , and the Freundlich exponent n . Both parameters can be varied for different soil horizons.

Anionic substances can be transported more rapidly through soil by using anion exclusion, as defined by the equation:

$$\theta_{mi(m)} = \theta_{mi} - \theta_{ae}, \quad (3)$$

where $\theta_{mi(m)}$ represents the fraction of water in the micropores available for transport, θ_{mi} is the total water content in the micropores, and θ_{ae} is the fraction of water in the micropores that is excluded from the calculation of mobile water [32].

The solute degradation is calculated by a first-order equation, which can be specified within four different domains: micro- or macropores of the liquid or solid phase. The degradation rates of the four domains μ_d are calculated by

$$\mu_D = \mu_{ref,D} \cdot F_w \cdot F_t, \quad (4)$$

where $\mu_{ref,D}$ represents different reference rate coefficients in different domains, which can be influenced by two factors: F_w dependent on the water content and F_t dependent on the temperature. In our simulations, both factors were set to 1, indicating no influence on the transformation rate.

Not-recovered masses associated with non-extractable residues (NER) account for masses that cannot be recovered by the extraction method. Within the model, a workaround was established by using the first-order equations

for degradation. Previous studies with PFAA [20] and pharmaceuticals [19] have shown that this approach is suitable for some use cases. The process was modeled using the degradation sink term U (mass/(m³·days)) given by

$$U = (1 - f) \cdot s_{mi} \cdot Y \cdot \mu_{(s),mi}, \quad (5)$$

with the solute concentration in the solid phase of micropores s_{mi} (mass/mass), the soil bulk density Y (mass/m³), and the degradation rate in the solid phase of micropores $\mu_{(s),mi}$ (1/days). Only sorption sites of micropores $(1 - f)$, where f is the fraction of macropores' sorption sites, were used.

The conversion factor for determining the mass of transformed substances is the formation fraction ff , which represents the relative fraction of a specific metabolite in relation to the entire transformed substance.

2.3 Model Parameterization

In the MACRO model, a lysimeter setup with free flow at the bottom outlet and variable water input at the top (Table S4) was used as the boundary condition. The model was parametrized using a combination of (1) measured values, (2) literature values, (3) calculations in MACRO, (4) default MACRO values, and (5) calculations outside the model, as listed in Table S14 to S17 (SI). The soil properties, including sand, clay and silt fractions, pH value, and OC content were obtained from measured values (Table S3, SI) with interpolation to reach 100%. The remaining soil properties were either calculated using the MACRO internal pedotransfer function ("footprint") or default values were used. The soil was divided into two different soil horizons with a total of one hundred numerical layers, each having a height of 0.5 cm.

The water input for the simulations was achieved through precipitation following the watering protocol of the column experiment. For the PFCA variant, the first water input was done simultaneously with PFCA mass input. In the diPAP variants, the substance masses were mixed into the soil before filling the columns. To incorporate mass input into the model, initial concentrations of the substance in the soil water were set, which depended on the substance parameters (adsorption) and required iterative approximation before each model run.

About 40% (440 mm/year) of the applied water (1,100 mm/year) was missing from the water balance and was related to evaporation. No seasonality was observed in the water balance. To account for the missing water, half of the evaporation was assumed at the top of the soil columns and half was related to the bottom of the soil columns since both were not waterproof.

The initial soil water content of both soil layers was each used for calibrating the water flow, while substance-related parameters were used to optimize the leaching and transformation of PFAS. Anion exclusion was used as a parameter since PFCA and diPAP are anionic in soil within the given pH range. Short-chain PFCA, in particular, have almost no retention in soil and could be affected by faster transport due to anion exclusion. The estimation of the distribution coefficient K_D was performed using the following equation [33]:

$$K_D = K_{OC} \cdot f_{OC} + K_{MIN} \cdot f_{S+C}, \quad (6)$$

where f_{OC} represents the organic carbon content and f_{S+C} represents the mineral content, K_{OC} is the normalized sorption coefficient for organic carbon, and K_{MIN} is the normalized sorption coefficient for mineral content (clay and silt). The equation was specified as applicable for PFSA and PFCA with a fluorinated carbon chain length ranging from 3 to 11 [33]. The sorption coefficients were obtained from the literature [33], and calculated values with an uncertainty of +25% were taken as initial upper bounds. The lower bounds were set to zero. In the simulation study, kinetic sorption was neglected based on results of Gassmann et al. [20].

In the PFCA variant of the soil column study, all transformation products were fully recovered except for PFOA (standard deviations were considered). Therefore, the formation of NER was only simulated for PFOA. In the diPAP variants, missing amounts in the molar balance were also observed. Only the diPAP amount that could be linked to observed metabolites (PFCA') or was still adsorbed to soil particles at the end of study was taken as substance input, as it was not possible to distinguish between NER, intermediate transformation products that were not identified and substance loss due to experimental issues such as sorption on materials. The transformation of diPAP was modeled using the liquid substance phase only. K_D , Freundlich n , anion exclusion θ_{ae} , formation of NER $\mu_{ref,s,mi}$ (applicable only for PFOA), and the transformation rate in the liquid phase $\mu_{ref,l,mi}$ were varied within a parameter range (Table 2). The

Table 2 Boundaries of parameters included in PFAS optimization

	K_D	Freundlich n	θ_{ae}	$\mu_{ref,s,mi}$	$\mu_{ref,l,mi}$
PFAS	l/kg	–	%	1/day	1/day
PFBA	0–0.17	0.7–1.0	0–15	–	–
PFPeA	0–0.39	0.7–1.0	0–15	–	–
PFHxA	0–0.95	0.7–1.0	0–15	–	–
PFHpA	0–2.14	0.7–1.0	0–15	–	–
PFOA	0–4.93	0.7–1.0	0–15	0–0.01	–
6:2 diPAP	1–100	0.7–1.0	0–15	–	0–1
8:2 diPAP	1–100	0.7–1.0	0–15	–	0–1

K_D distribution coefficient, θ_{ae} anion exclusion, $\mu_{ref,s,mi}$ NER formation in the solid phase of the micropores, $\mu_{ref,l,mi}$ transformation rate in the liquid phase of the micropores

Freundlich n was varied within the range of 0.7 to 1, values above 1 were not considered due to the approach used, which stated that sorption decreases with concentration, in accordance with the results of Gellrich [34]. The lower value of 0.7 was chosen based on the results of Gassmann et al. [20].

2.4 Evaluation of Model Performance, Optimization Algorithm, and Modeling Strategy

2.4.1 Goodness-of-fit Values

The Kling-Gupta-Efficiency (*KGE*) [35] was used as the objective function to evaluate the goodness-of-fit for the substance simulations in the percolate m compared to the 52 observations o . The *KGE* is given by

$$KGE_x = 1 - \sqrt{(r_x - 1)^2 + (\alpha - 1)^2 + (\beta - 1)^2} \quad (7)$$

$$\alpha = \frac{s_x(m)}{s_x(o)}, \beta = \frac{\overline{m_x}}{\overline{o_x}}, \quad (8)$$

using the Pearson correlation coefficient of simulated values r_x , the standard deviation s_x , the average of simulated values $\overline{m_x}$, and the average of observed values $\overline{o_x}$.

The root-mean-square-error (*RMSE*) is given by

$$RMSE = \sqrt{\frac{1}{n} \sum_{t=1}^n (m_t - o_t)^2}, \quad (9)$$

and was used as an objective function to evaluate the goodness-of-fit between modeled substance masses m_t and observed substance masses o_t in the different soil layers (4 observations) and in the percolate (52 observations) at each time step t . The *RMSE* has the advantage to enhance the influence of high absolute errors, which was more crucial than relative errors. Both *KGE* and *RMSE* were calculated using the hydroGOF (0.4–0) package in GNU R.

KGE (mass in percolate) and *RMSE* (mass in soil) were used in the PFCA simulation study, and *RMSE* (mass in percolate, mass in soil) was used in the diPAP simulation.

2.4.2 Optimization, Uncertainty Ranges, and Best Compromises

The optimization was performed using the global evolutionary algorithm caRamel [29], which was implemented in the GNU R environment in “caRamel” version 1.3. The algorithm creates a basic population with sets of parameter values within defined boundaries. Through various processes, such as mutation, a new generation is created from individual update processes. This algorithm optimizes two objective functions at the same time, which corresponds

to the substance mass in leaching water and the substance mass in soil in this study. The result of this multiobjective optimization is a pareto front with equally good parameter sets (trade-offs), which gives an uncertainty boundary of the predictive model.

To choose the behavioral models for uncertainty assessment from all simulations, we used thresholds for both objectives instead of using all parameter sets of the pareto front. This practice allows to include parameter sets with acceptable trade-offs (Fig. 1), while neglecting extreme trade-offs at the borders of the pareto front. In the PFCA-study, the thresholds were set to $(KGE_{thres,min}, RMSE_{thres,max}) = (0.8, 3.1 \mu\text{g}/\text{soil layer})$. The RMSE threshold was developed by taking 0.5 Ma-% of the initially applied mass as a maximum deviation. In the diPAP studies, thresholds were set to $(RMSE_{thres,min}, RMSE_{thres,max}) = (0, 5.8 \mu\text{g}/\text{soil layer})$ using the same approach for the maximum RMSE in soil. RMSE of diPAP in percolate was set to zero as a hard criterion, because diPAP above the limit of quantification (LOQ) was not detected in either the lowest soil layer or the percolate.

The best compromise using the example PFCA is given by

$$\min(d(A_i; A_{opt})) = \left(\left(\frac{KGE_i - 1}{\frac{d_{max,KGE}}{RMSE_i - 0}} \right)^2 + \left(\frac{RMSE_i}{3.1} \right)^2 \right)^{1/2} \tag{10}$$

and represents the point on the pareto front closest [29] to the optimal solution $A_{opt} = (KGE_{opt}, RMSE_{opt})$ or

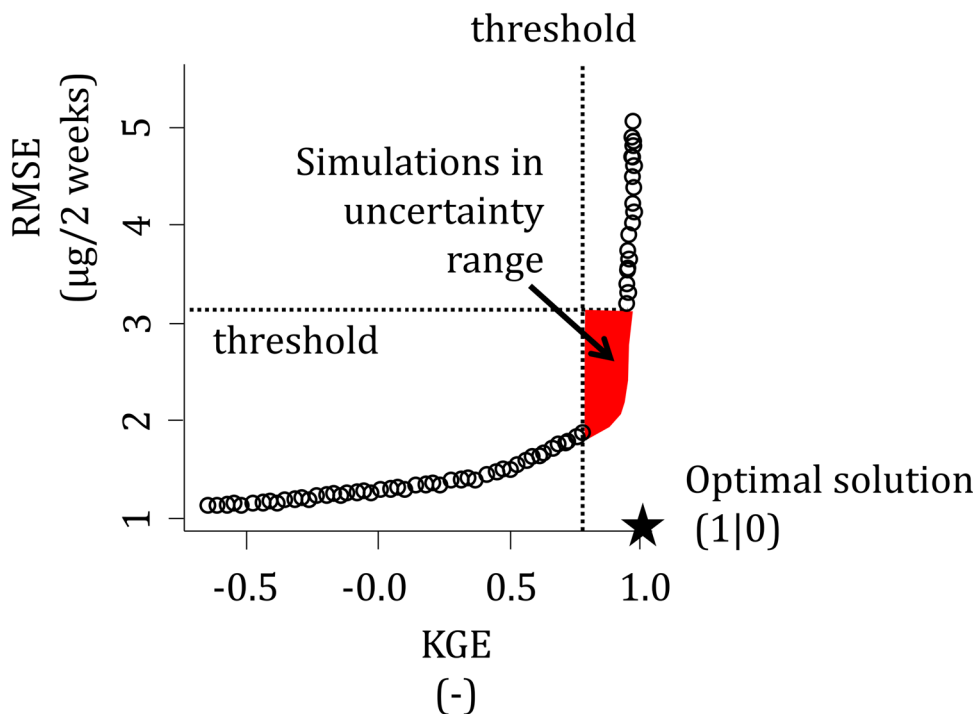
$A_{opt} = (RMSE_{opt}, RMSE_{opt})$, respectively, with the maximum distance d_{max} used for scaling.

2.4.3 Modeling Strategy

The water flow calibration was the first step for all simulation studies (Fig. 2), which involved determining the initial soil water contents of the lower and the upper soil as parameters. A total of 1000 random parameter sets, each with varying initial soil moisture of lower and upper soil, were evaluated based on their RMSE and KGE values. The best parameter set was chosen and fixed for subsequent substance optimizations. Water flow was separated from the substance optimization to allow for comparable results of optimized substance parameters. In the second step, PFCA masses in soil and percolate were optimized simultaneously using 15,000 simulations.

In the third step, two modeling approaches for diPAP transformation and metabolite leaching were investigated. In strategy 1, a constant biotransformation rate in the liquid phase of the micropores ($\mu_{mi,l} = \mu_{ref,mi,l}$) was assumed. After optimizing diPAP transformation (7,500 simulations), three simulations were performed using parameters at their maximum/minimum values as well as the best compromise, which were obtained separately from the PFCA optimization. These parameters were then used to simulate metabolites. In strategy 2, the biotransformation rate of diPAP ($\mu_{mi,l} = \mu_{ref,mi,l}$) was manually altered at a specific date to test the hypothesis that it decreased from high to low after a

Fig. 1 Exemplary representation of the parameter selection from the Pareto front using thresholds



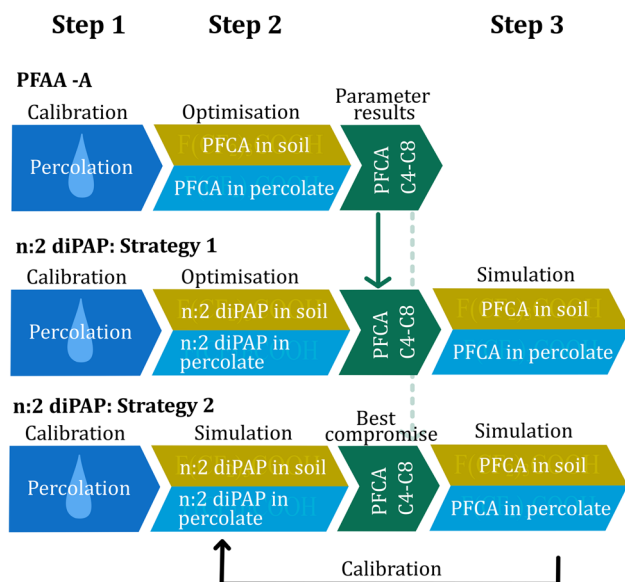


Fig. 2 Model strategy. The optimization of PFAS in soil and percolate is done simultaneously. The optimization of n:2 diPAP follows two different strategies: biotransformation rate $\mu_{mi,i}$ is constant (strategy 1), biotransformation rate decreases at a specific date (strategy 2)

certain time, which could be attributed to various factors such as soil water content or oxygen levels [36] whereby at a high soil water content there is less space for air-filled pores. The subsequent metabolite simulation was performed with parameters from the best compromise of the PFCA-study. These results were then used to calibrate the transformation rates of the precursors again. Automatic calibration could not be used, because the MACRO command line version does not support time-dependent parameter changes. Therefore, the transformation rate changes were done manually using the graphical interface of MACRO.

3 Results and Discussion

3.1 PFCA Leaching

The water flow calibration in the PFCA study resulted in satisfactory objective function values ($RMSE$: 4.7 ml/column, KGE : 0.89 (-)). Especially the first percolation values were well reproduced, reducing modeling errors in short-chain PFCA leaching, because their leaching occurred in a tight time frame. Substance leaching was optimized to obtain good fits with $KGE > 0.8$ (-) and $RMSE < 3.1$ $\mu\text{g}/\text{soil layer}$, resulting in parameter ranges and a best compromise parameter set (Table 3). The K_D value increased with increasing carbon chain length, consistent with previous studies [33, 37, 38]. Our optimized K_D values are much lower than the initially used values, which were calculated according to Fabregat-Palau et al. [33]. This could be due to the high

Table 3 Parameter values of best compromises after optimization (parameter range of behavioral models) of five PFCA using 15,000 simulation runs. PFBA ($n=5402$), PFPeA ($n=9231$), PFHxA ($n=9186$), PFHpA ($n=8423$), and PFOA ($n=1258$) with n =number of behavioral models

	K_D (l/kg)	Freundlich n (-)	θ_{ae} (%)	$\mu_{ref,s,mi}$ ($10^{-3}/\text{days}$)
PFBA	0.01 (0.00–0.05)	0.8 (0.7–1.0)	10.7 (6.9–13.9)	–
PFPeA	0.05 (0.00–0.06)	1.0 (0.8–1.0)	15.0 (8.6–15.0)	–
PFHxA	0.08 (0.00–0.10)	1.0 (0.7–1.0)	15.0 (1.9–15.0)	–
PFHpA	0.14 (0.02–0.21)	1.0 (0.7–1.0)	15.0 (0.0–15.0)	–
PFOA	0.50 (0.42–0.63)	0.9 (0.7–1.0)	0.0 (0.0–11.0)	2.7 (1.5–4.4)

K_D distribution coefficient, θ_{ae} anion exclusion, $\mu_{ref,s,mi}$ NER formation in the solid phase of the micropores

mass of PFAA used (10 PFAA \times 623 μg), which could enhance their mobility compared to soil columns studies with less mass input [39]. This may be particularly relevant in real contamination cases where other co-contaminants are present, as shown in Zhang et al. for hydrocarbon surfactants [40]. The NER formation rate of PFOA ranged from 0.0015 to 0.0044 1/day which is comparable to the results obtained by Gassmann et al. [20], who modeled PFOA leaching in an undisturbed lysimeter using MACRO.

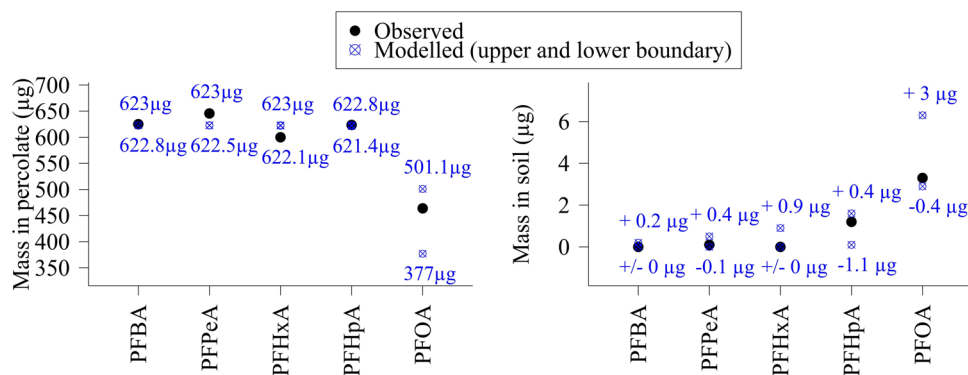
The modeled values of mass output and mass retention fit well with the observed values (Fig. 3), with PFOA showing the largest deviations, which are still within an acceptable range. In some cases, the observed values of masses were higher than the initially applied masses of 623 μg according to analytic results, which could be due to uncertainties. In these cases, perfect fits by modeled values are impossible, which weakens the shown deviation between observed and modeled values, as is the case with PFPeA.

3.2 diPAP Transformation and Related PFCA Leaching

3.2.1 Re-analysis of Soil Column Experiment

An additional analysis of the soil column experiment data was conducted to derive a hypothesis on diPAP transformation leading to simulation strategy 2. A comparison of the discharge dynamics of PFCA and PFCA' (PFCA as a metabolite of diPAP) showed similar leaching behavior (Fig. 4), despite the fact that PFCA' was formed by diPAP transformation first. An analysis of the spiked soil prior the experiment showed negligible amounts of transformation products in the 6:2 diPAP study (1.1 μg PFPeA, 1.3 μg PFHxA) as well as in the 8:2 diPAP study (1.6 μg PFOA), which cannot account for the amounts found in the percolate. These results also indicate that bacteria had already adjusted to the conditions, and a lag time of biotransformation [41] was not visible in the results of substance leaching, as the leaching curves were similar

Fig. 3 Comparison of observed values and upper and lower modeled values of uncertainty ranges PFCA. Comparison of maximal and minimal masses (μg) in percolate (left) and maximal and minimal absolute differences (μg) of masses in soil (right). Initial mass of each PFCA was $623 \mu\text{g}$



to those from the PFAA study with no biotransformation. In contrast to PFCA leaching, a consistent but small amount of PFCA' was found in the percolate until the end of both diPAP studies, indicating ongoing transformation and desorption. The deviation between the curves after the decline could be the result of ongoing production and leaching of transformation products. This behavior led to the hypothesis that the majority of the measured PFCA' was formed before the water content reached an almost constant level. This assumption was supported by the leaching curves of PFPeA and PFOA (Fig. 4), as well as other PFCA metabolites (Figure S1, SI) and could be related to the soil moisture content or oxygen availability in soil, as these are parameters that could have changed after start of the study. Other studies have shown that high soil moisture "near full saturation" can have a suppressive effect on biotransformation by limiting the oxygen available to microorganisms [42].

There is evidence that the transformation of diPAP depends on the surrounding conditions. In experiments where 6:2 and 8:2 diPAP were mixed into soil and then filled into columns [10] and lysimeters [43], the results varied greatly between the column study with controlled conditions and the lysimeter study with near-natural conditions. The half-lives (DT50) of both diPAP were higher under near-natural conditions than under controlled conditions in the column study, where the temperature was around 20°C and the water input was constant at a weekly level. The soil water content is known to have an influence on diPAP degradation

by providing OH-radicals for the hydrolysis of phosphate ester bonds to fluorotelomer alcohol (FTOH) [44]. Additionally, oxygen has been shown to enhance the transformation of diPAP intermediates. For example, a comparison of aerobic and anaerobic conditions of 8:2 FTOH showed that the transformation rate was ten times faster under aerobic conditions than under anaerobic conditions in a batch test with activated sludge [45].

3.2.2 Strategy 1: Constant Biotransformation Rate

Initially, modeling the behavior of diPAP was performed using a uniform transformation rate. The best compromises had *RMSE* values of $3.6 \mu\text{g}/\text{soil layer}$ (6:2 diPAP) and $34.2 \mu\text{g}/\text{soil layer}$ (8:2 diPAP). The deviations of 8:2 diPAP were far above the chosen threshold of $5.8 \mu\text{g}/\text{soil layer}$ and could not be improved through parameter adjustments. Therefore, thresholds and parameter boundaries were only determined for 6:2 diPAP. For 8:2 diPAP, simulations were selected, all of which had a d_{max} value of 5.7 (-) (Table 4). Other PFAS tend to have a decrease in solubility and, therefore, a decrease in sorptivity with an increase in chain length within a group of similar compounds [46]. It is noteworthy that the K_D values of best compromises of 8:2 diPAP are lower than for 6:2 diPAP, which is the opposite trend expected for PFAS. However, it should be noted that there is a large range of K_D values.

There are different possible combinations of substance parameters with equally good results of soil substance content.

Fig. 4 Comparison of observed PFCA masses in the percolate ($\mu\text{g}/2$ weeks) applied as pure substance and their respective transformation products of n:2 diPAP. Left: PFPeA and PFPeA' (transformation product of 6:2 diPAP). Right: PFOA and PFOA' (transformation product of 8:2 diPAP)

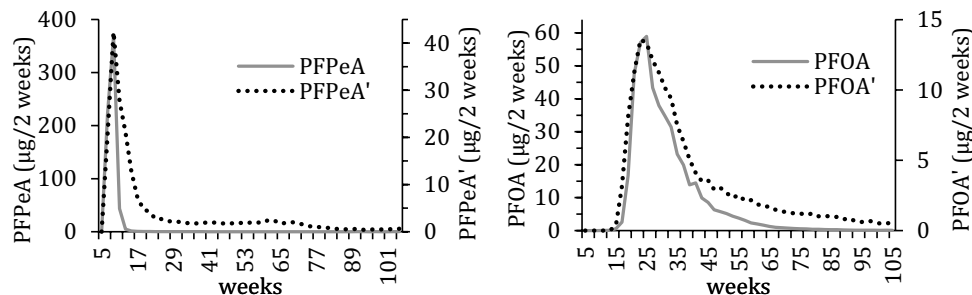


Table 4 Parameter values of best compromise (behavioral models) of 6:2 diPAP and the best compromise ($d_{max} \leq 5.7$) of 8:2 diPAP using 7500 simulation runs. 6:2 diPAP ($n=6205$) and 8:2 diPAP ($n=2391$) with n =number of behavioral models

	K_D (l/kg)	Freundlich n (-)	θ_{ae} (%)	$\mu_{ref,l,mi}$ (10^{-3} /days)
6:2 diPAP	39.24 (16.43–44.42)	1.00 (0.82–1.00)	0.7 (0–8.4)	579.3 (456.9–1000)
8:2 diPAP	30.42 (26.35–31.69)	1.00 (0.95–1.00)	6.7 (3.8–12.4)	89.6 (81.2–114.4)

K_D distribution coefficient, θ_{ae} anion exclusion, $\mu_{ref,l,mi}$ transformation rate in the liquid phase of the micropores

In each case, the degradation curve showed similar characteristics. Therefore, we considered it sufficient to use one parameter set for the basic simulation, which provides the input values for the transformation product (PFCA') simulation.

However, the leaching dynamics of the transformation products found in the percolate were not adequately

represented, as exemplified by PFPeA' and PFOA' and their best parameter sets (Fig. 5, Strategy 1). The leaching dynamics of the other PFCA' are shown in Fig. S7-S9 (SI). The peaks were underestimated, suggesting that too little diPAP mass was transformed before the first percolation. The falling limb after the sharp peak of the substances mass in the leachate was overestimated, which may be attributed to a too high continuous first order transformation. Furthermore, using the most mobile parameters of the PFCA showed no considerable improvement for both metabolites.

3.2.3 Strategy 2: Variable Biotransformation Rate

It was investigated to what extent the dynamics of metabolites, which could not be represented by a uniform transformation rate of the precursor, could be modeled using two different transformation rates. For this purpose, a fast transformation rate was applied until the beginning of July 2019, followed by a lower rate. The dates chosen correspond to

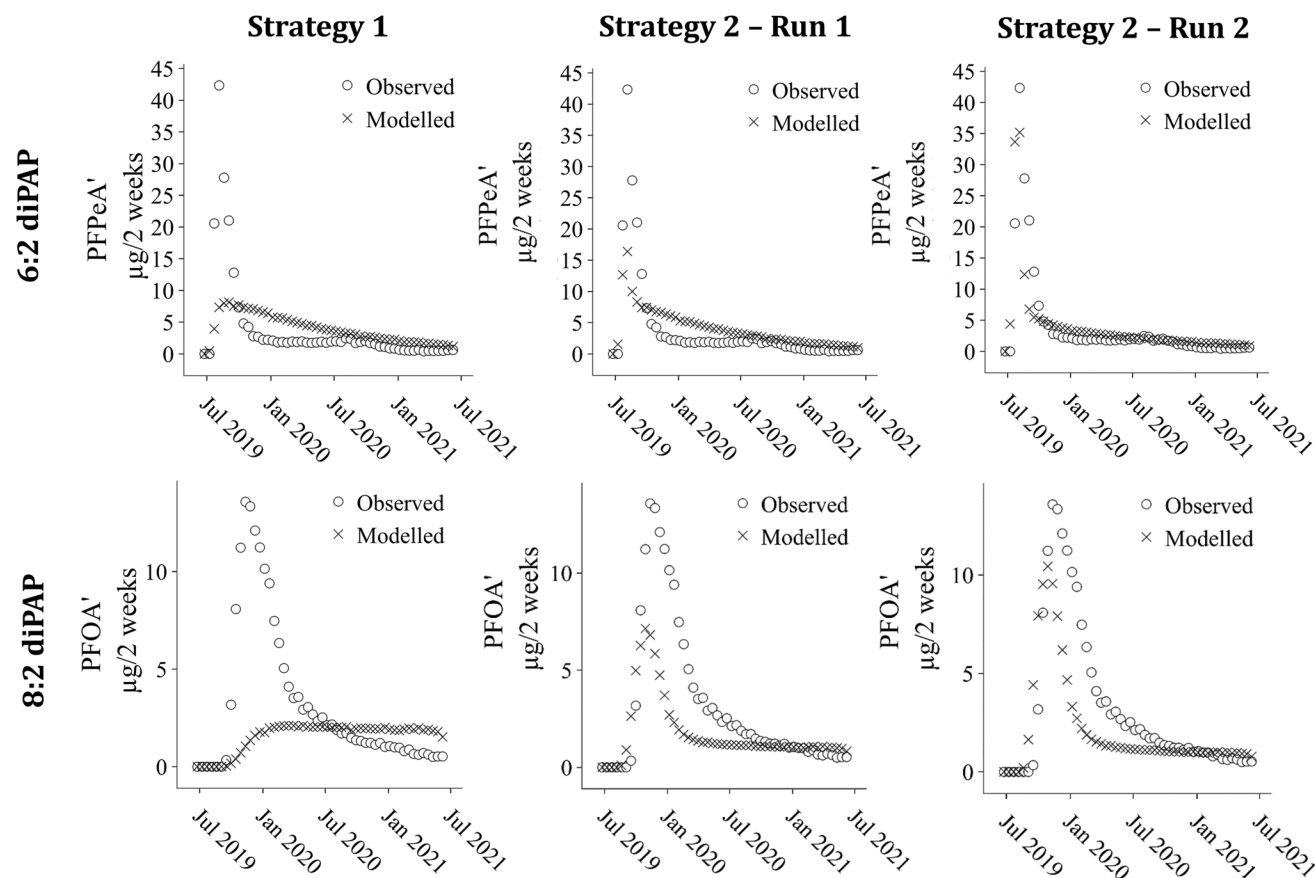


Fig. 5 Leaching of PFPeA' (6:2 diPAP) and PFOA' (8:2 diPAP) in $\mu\text{g}/2$ weeks using modeling strategy 1 (uniform biotransformation) and strategy 2 (fast biotransformation followed by slow biotransformation). Comparison of modeled and observed values ($\mu\text{g}/2$ weeks). Substance parameters correspond to best compromises of PFCA-study (see Table 3). Biotransformation rates liquid phase of 6:2 diPAP: 0.5791/days (strategy 1, $RMSE$: 6.7 $\mu\text{g}/2$ weeks), 2 and 0.6

1/days (strategy 2, run 1, $RMSE$: 5.2 $\mu\text{g}/2$ weeks), and 6 and 0.45 1/days (strategy 2, run 2, $RMSE$: 3.8 $\mu\text{g}/2$ weeks). Biotransformation rates liquid phase of 8:2 diPAP: 0.109 1/days (strategy 1, $RMSE$: 4.1 $\mu\text{g}/2$ weeks), 2 and 0.05 1/days (strategy 2, run 1, $RMSE$: 2.9 $\mu\text{g}/2$ weeks), and 3 and 0.05 1/days (strategy 2, run 2, $RMSE$: 2.6 $\mu\text{g}/2$ weeks)

the days after which a soil water equilibrium between input and output was observed, based on modeling results around the date of July 3, 2019. A variation of these dates had an impact on the leaching curves of the transformation products (Fig. 6), particularly on the peak, which was higher when the transformation rate was longer at a higher level. Even a two-day extension had already a noticeable effect on the peak, resulting in an increase of 4 $\mu\text{g}/2$ weeks. This demonstrates the high sensitivity of transformation rate change dates on the modeled leaching curves.

Overall, the first transformation rate influenced the peak of metabolite output and the second transformation rate influenced the slow metabolite tailing after the peak. A comparison of metabolite outputs of both strategies is shown in Fig. 5 (Strategy 2) for PFPeA' and PFOA' and for the other PFCA in Figures S7 to S9 (SI). However, in some cases, the peaks were overestimated. These deviations could have occurred due to uncertainties such as (1) the use of a mean value from three structurally identical soil columns for each diPAP study, (2) sample analytics, (3) substance parameters, and (4) the date of transformation rate change. Nevertheless, it was shown that the time periods of specific transformation rates can be chosen differently and still produce similar results. Furthermore, other parameter combinations for the diPAP are possible, but they would require different calibrated transformation rates to be able to represent the transformation products to the same extent. For this reason, no generality of the substance parameters and transformation rates is intended to be conveyed here. However, the study provided evidence that the transformation

rates of the diPAP can be greatly affected by certain external influences.

Possible influences on the high amounts of PFCA' in the first weeks of the study could be related to favorable conditions for transformation, with water and oxygen available for hydrolysis and microbial transformation. After some weeks, the oxygen transfer into the soil could have decreased, and the transformation into PFCA' could have slowed down due to the water content approaching the saturation limit. The relationship between soil moisture, oxygen, and transformation rate has been established for substances such as pesticides [47, 48], petroleum hydrocarbon [49], and chlorophenol [42]. However, the minimal and optimal water content [42, 48, 49] and the effect of additional factors such as microorganisms, salinity, bioavailability, pH, and nutrients can vary among different substances [49]. It is worth noting that the approach used in MACRO (Eq. 4) to calculate the transformation rate based on soil water content was not considered in this study. Similar to other leaching models [50], this approach [51] assumes that the optimal transformation occurs at high water content and does not consider any decrease in the transformation rate at high water contents.

Further investigations are needed to improve the predictions of real contamination cases by examining the transformation of diPAP under different conditions. If the transformation rate indeed decreases with increasing soil moisture, then high transformation rates would be expected to occur mainly in the upper vadose zone, where precursors are already found in agricultural areas [8].

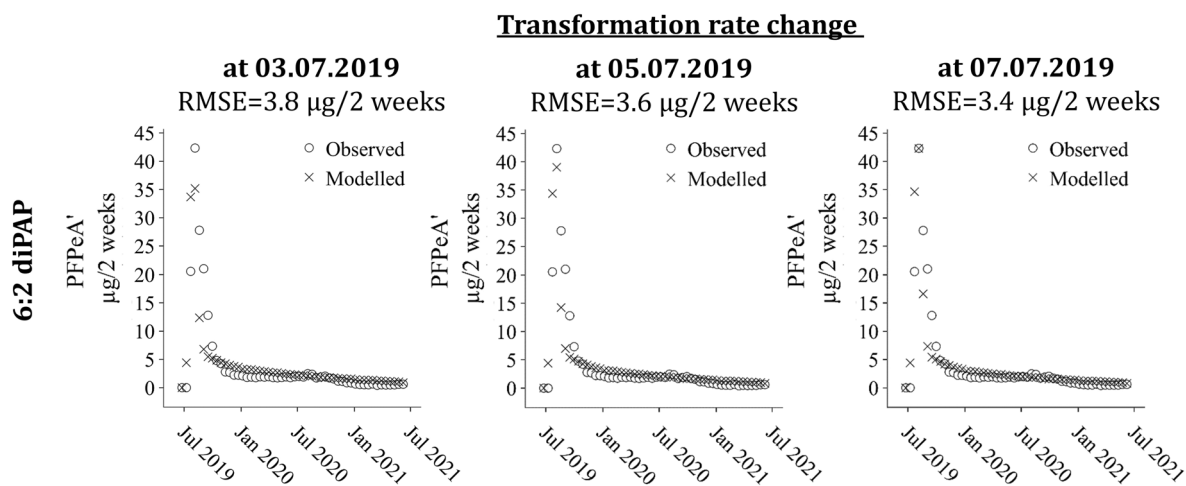


Fig. 6 Leaching of PFPeA' (6:2 diPAP) using modeling strategy 2 (fast biotransformation followed by slow biotransformation) and the influence of varying the transformation rate change date. Comparison

of modeled and observed values ($\mu\text{g}/2$ weeks). Substance parameters correspond to best compromises of PFCA-study (see Table 3). Bio-transformation rates liquid phase: 6 and 0.45 1/days (strategy 2, run 2)

4 Conclusions

Given their ubiquitous occurrence in the environment, PFAS have been the subject of numerous simulation studies aimed at describing their behavior in the environment. This study focuses particularly on the precursors of the non-degradable compounds, which were successfully simulated using MACRO. Evidence suggests that the transformation of diPAP into persistent PFAS is affected by non-stationary parameters, with soil moisture being a possible candidate. The use of a drastic decrease in the biotransformation rate after almost reaching an equilibrium water flow resulted in a good model performance. Whether soil water content or another parameter, such as oxygen level, is the influencing factor needs to be evaluated by performing studies that focus on the effects of environmental parameters on biotransformation of diPAP.

Supplementary Information The online version contains supplementary material available at <https://doi.org/10.1007/s10666-023-09936-8>.

Acknowledgements Special thanks are due to all project partners of the project PROSPeCT and the developers of MACRO, Nicolas Jarvis and Mats Larsbo, also for putting the model as open access.

Author Contributions Eva Weidemann wrote the original draft, prepared all figures and tables, wrote the code used in the simulation study, prepared the conceptualization, conducted the simulation study and analyzed the data. Matthias Gassmann reviewed and edited the manuscript and supported all steps above.

Funding Open Access funding enabled and organized by Projekt DEAL. This study was funded by the Ministry of the Environment, Climate Protection and the Energy Sector Baden-Württemberg (Germany) through the Project “PROSPeCT-PFAA and Precursors Soil Plant Contamination” (FKZ BWPFC19002, FKZ BWPFC19004, FKZ BWPFC19005, and FKZ BWPFC19006).

Availability of Data and Materials The datasets generated or used in this study are available from the corresponding author on reasonable request or are included in this published article and its supplementary information (SI).

Declarations

Ethics Approval Not applicable.

Competing Interests The authors declare no competing interests.

Open Access This article is licensed under a Creative Commons Attribution 4.0 International License, which permits use, sharing, adaptation, distribution and reproduction in any medium or format, as long as you give appropriate credit to the original author(s) and the source, provide a link to the Creative Commons licence, and indicate if changes were made. The images or other third party material in this article are included in the article’s Creative Commons licence, unless indicated otherwise in a credit line to the material. If material is not included in the article’s Creative Commons licence and your intended use is not permitted by statutory regulation or exceeds the permitted use, you will need to obtain permission directly from the copyright holder. To view a copy of this licence, visit <http://creativecommons.org/licenses/by/4.0/>.

References

1. US Environmental Protection Agency. (2021). PFASIEPA: PFAS structures in DSSTox (update August 2021). <https://comptox.epa.gov/dashboard/chemical-lists/PFASSTRUCTV4>. Accessed 15 Jun 2022.
2. Cousins, I. T., DeWitt, J. C., Glüge, J., Goldenman, G., Herzke, D., Lohmann, R., Ng, C. A., Scheringer, M., & Wang, Z. (2020). The high persistence of PFAS is sufficient for their management as a chemical class. *Environmental Science. Processes & Impacts*, 22, 2307–2312. <https://doi.org/10.1039/d0em00355g>
3. ECHA. (2020). Pentadecafluorooctanoic acid - substance information. <https://echa.europa.eu/de/substance-information/-/substanceinfo/100.005.817>. Accessed 24 Jun 2020.
4. Lee, H., D’eon, J., & Mabury, S. A. (2010). Biodegradation of polyfluoroalkyl phosphates as a source of perfluorinated acids to the environment. *Environmental Science and Technology*, 44, 3305–3310. <https://doi.org/10.1021/es9028183>
5. Zweigle, J., Bugsel, B., Schmitt, M., & Zwiener, C. (2021). Electrochemical oxidation of 6:2 polyfluoroalkyl phosphate diester-simulation of transformation pathways and reaction kinetics with hydroxyl radicals. *Environmental Science and Technology*. <https://doi.org/10.1021/acs.est.1c02106>
6. Yao, Y., Zhao, Y., Sun, H., Chang, S., Zhu, L., Alder, A. C., & Kannan, K. (2018). Per- and polyfluoroalkyl substances (PFASs) in indoor air and dust from homes and various micro-environments in China: Implications for human exposure. *Environmental Science and Technology*, 52, 3156–3166. <https://doi.org/10.1021/acs.est.7b04971>
7. Lee, H., & Mabury, S. A. (2011). A pilot survey of legacy and current commercial fluorinated chemicals in human sera from United States donors in 2009. *Environmental Science and Technology*, 45, 8067–8074. <https://doi.org/10.1021/es200167q>
8. Bugsel, B., & Zwiener, C. (2020). LC-MS screening of poly- and perfluoroalkyl substances in contaminated soil by Kendrick mass analysis. *Analytical and Bioanalytical Chemistry*, 412, 4797–4805. <https://doi.org/10.1007/s00216-019-02358-0>
9. Wang, Z., MacLeod, M., Cousins, I. T., Scheringer, M., & Hungerbühler, K. (2011). Using COSMOtherm to predict physicochemical properties of poly- and perfluorinated alkyl substances (PFASs). *Environmental Chemistry*, 8, 389. <https://doi.org/10.1071/EN10143>
10. Weidemann, E., Lämmer, R., Stahl, T., Göckener, B., Bücking, M., Breuer, J., Kowalczyk, J., Just, H., Boeddinghaus, R. S., & Gassmann, M. (2022). Leaching and transformation of PFAA and diPAP in unsaturated soil column studies. *Environmental Toxicology and Chemistry*. <https://doi.org/10.1002/etc.5417>
11. Just, H., Göckener, B., Lämmer, R., Wiedemann-Krantz, L., Stahl, T., Breuer, J., Gassmann, M., Weidemann, E., Bücking, M., & Kowalczyk, J. (2022). Degradation and plant transfer rates of seven fluorotelomer precursors to perfluoroalkyl acids and F-53B in a soil-plant system with maize (*Zea mays* L.). *J Agric Food Chem*. <https://doi.org/10.1021/acs.jafc.1c06838>
12. Rovero, M., Cutt, D., Griffiths, R., Filipowicz, U., Mishkin, K., White, B., Goodrow, S., & Wilkin, R. T. (2021). Limitations of current approaches for predicting groundwater vulnerability from PFAS contamination in the vadose zone. *Ground Water Monit Remediat*, 41, 62–75. <https://doi.org/10.1111/gwmm.12485>
13. Brusseau, M. L., Anderson, R. H., & Guo, B. (2020). PFAS concentrations in soils: Background levels versus contaminated sites. *Science of the Total Environment*, 740, 140017. <https://doi.org/10.1016/j.scitotenv.2020.140017>
14. Larsbo, M., Jarvis, N. (2003). MACRO 5.0: a model of water flow and solute transport in macroporous soil: technical description, Uppsala.

15. The HYDRUS code for simulating the one-dimensional movement of water, heat, and multiple solutes in variably-saturated media. Version 6.0. (1998).
16. Vanclooster, M., Boesten, J., Trevisan, M., Brown, C. D., Capri, E., Eklo, O. M., Gottesbüren, B., Gouy, V., & van der Linden, A. (2000). A European test of pesticide-leaching models: Methodology and major recommendations. *Agricultural Water Management*, *44*, 1–19. [https://doi.org/10.1016/S0378-3774\(99\)00081-5](https://doi.org/10.1016/S0378-3774(99)00081-5)
17. García-Santiago, X., Garrido, J. M., Lema, J. M., & Franco-Uría, A. (2017). Fate of pharmaceuticals in soil after application of STPs products: Influence of physicochemical properties and modelling approach. *Chemosphere*, *182*, 406–415. <https://doi.org/10.1016/j.chemosphere.2017.05.049>
18. Jalali, M., Farahani, E. A., & Jalali, M. (2022). Simulating phosphorus leaching from two agricultural soils as affected by different rates of phosphorus application based on the geochemical model PHREEQC. *Environmental Monitoring and Assessment*, *194*, 164. <https://doi.org/10.1007/s10661-022-09828-6>
19. Spill, C., & Gassmann, M. (2022). Long-term Sulfamethazine (SMZ) leaching simulation in two different soils using the MACRO model. *Journal of Environmental Quality*. <https://doi.org/10.1002/jeq2.20337>
20. Gassmann, M., Weidemann, E., & Stahl, T. (2021). Combined leaching and plant uptake simulations of PFOA and PFOS under field conditions. *Environmental Science and Pollution Research*, *28*, 2097–2107. <https://doi.org/10.1007/s11356-020-10594-6>
21. Brusseau, M. L. (2020). Simulating PFAS transport influenced by rate-limited multi-process retention. *Water Research*, *168*, 115179. <https://doi.org/10.1016/j.watres.2019.115179>
22. Silva, J. A. K., Šimůnek, J., & McCray, J. E. (2020). A modified HYDRUS model for simulating PFAS transport in the vadose zone. *Water*, *12*, 2758. <https://doi.org/10.3390/w12102758>
23. Raschke, A., Nejadhashemi, A. P., & Rafiei, V. (2022). Overview of modeling, applications, and knowledge gaps for integrated large-scale PFAS modeling. *J Environ Eng*, *148*. [https://doi.org/10.1061/\(ASCE\)EE.1943-7870.0002033](https://doi.org/10.1061/(ASCE)EE.1943-7870.0002033)
24. Beven, K. (2006). A manifesto for the equifinality thesis. *Journal of Hydrology*, *320*, 18–36. <https://doi.org/10.1016/j.jhydrol.2005.07.007>
25. Katoch, S., Chauhan, S. S., & Kumar, V. (2021). A review on genetic algorithm: Past, present, and future. *Multimed Tools Appl*, *80*, 8091–8126. <https://doi.org/10.1007/s11042-020-10139-6>
26. Selman, B., & Gomes, C. P. (2005). Hill-climbing search. In: Nadel L (ed) *Encyclopedia of cognitive science*, vol 4. Wiley, Chichester, West Sussex Eng., Hoboken, N.J, 397.
27. Venter, G. (2010). Review of optimization techniques. In: Blockley R, Shyy W (eds) *Encyclopedia of aerospace engineering*, vol 156. Wiley Interscience, Hoboken, NJ, 215.
28. Zambrano-Bigiarini, M., & Rojas, R. (2013). A model-independent particle swarm optimisation software for model calibration. *Environmental Modelling & Software*, *43*, 5–25. <https://doi.org/10.1016/j.envsoft.2013.01.004>
29. Monteil, C., Zaoui, F., Le Moine, N., & Hendrickx, F. (2020). Multi-objective calibration by combination of stochastic and gradient-like parameter generation rules – the caRamel algorithm. *Hydrology and Earth System Sciences*, *24*, 3189–3209. <https://doi.org/10.5194/hess-24-3189-2020>
30. Forum for co-ordination of pesticide fate models and their use. (2000). FOCUS Groundwater Scenarios in the EU Review of Active Substances: Report of the FOCUS Groundwater Scenarios Workgroup EC Document Reference Sanco/321/ 2000-Rev.2. 202.
31. Larsbo, M. (2020). MACRO 5.2: MACRO a model of water flow and solute transport in macroporous soil. <https://www.slu.se/en/Collaborative-Centres-and-Projects/SLU-centre-for-pesticides-in-the-environment/models/macro-52/>. Accessed 2022.
32. Moeys, J., Larsbo, M., Bergström, L., Brown, C. D., Coquet, Y., & Jarvis, N. J. (2012). Functional test of pedotransfer functions to predict water flow and solute transport with the dual-permeability model MACRO. *Hydrology and Earth System Sciences*, *16*, 2069–2083. <https://doi.org/10.5194/hess-16-2069-2012>
33. Fabregat-Palau, J., Vidal, M., & Rigol, A. (2021). Modelling the sorption behaviour of perfluoroalkyl carboxylates and perfluoroalkane sulfonates in soils. *Science of the Total Environment*, *801*, 149343. <https://doi.org/10.1016/j.scitotenv.2021.149343>
34. Gellrich, V. (2014). Sorption and distribution of per- and polyfluorinated compounds in water and soil. Dissertation, Justus-Liebig-Universität.
35. Gupta, H. V., Kling, H., Yilmaz, K. K., & Martinez, G. F. (2009). Decomposition of the mean squared error and NSE performance criteria: Implications for improving hydrological modelling. *Journal of Hydrology*, *377*, 80–91. <https://doi.org/10.1016/j.jhydrol.2009.08.003>
36. Vidali, M. (2001). Bioremediation. *An overview. Pure and Applied Chemistry*, *73*, 1163–1172. <https://doi.org/10.1351/pac200173071163>
37. Milinovic, J., Lacorte, S., Vidal, M., & Rigol, A. (2015). Sorption behaviour of perfluoroalkyl substances in soils. *Science of the Total Environment*, *511*, 63–71. <https://doi.org/10.1016/j.scitotenv.2014.12.017>
38. Higgins, C. P., & Luthy, R. G. (2006). Sorption of perfluorinated surfactants on sediments. *Environmental Science and Technology*, *40*, 7251–7256. <https://doi.org/10.1021/es061000n>
39. Gellrich, V., Stahl, T., & Knepper, T. P. (2012). Behavior of perfluorinated compounds in soils during leaching experiments. *Chemosphere*, *87*, 1052–1056. <https://doi.org/10.1016/j.chemosphere.2012.02.011>
40. Zhang, Q., Wu, X., Lyu, X., Gao, B., Wu, J., & Sun, Y. (2022). Effects of anionic hydrocarbon surfactant on the transport of perfluorooctanoic acid (PFOA) in natural soils. *Environmental Science and Pollution Research*, *29*, 24672–24681. <https://doi.org/10.1007/s11356-021-17680-3>
41. Bertrand, R. L. (2019). Lag phase is a dynamic, organized, adaptive, and evolvable period that prepares bacteria for cell division. *J Bacteriol*, *201*. <https://doi.org/10.1128/JB.00697-18>
42. Cho, Y.-G., Rhee, S.-K., & Lee, S.-T. (2000). Effect of soil moisture on bioremediation of chlorophenol-contaminated soil. *Biotechnology Letters*, *22*, 915–919. <https://doi.org/10.1023/A:1005612232079>
43. Lämmer, R., Weidemann, E., Göckener, B., Stahl, T., Breuer, J., Kowalczyk, J., Just, H., Boeddinghaus, R. S., Gassmann, M., Kling, H.-W., & Bücking, M. (2022). Evaluation of the transformation and leaching behavior of two polyfluoroalkyl phosphate diesters in a field lysimeter study. *Journal of Agricultural and Food Chemistry*. <https://doi.org/10.1021/acs.jafc.2c03334>
44. Liu, C., & Liu, J. (2016). Aerobic biotransformation of polyfluoroalkyl phosphate esters (PAPs) in soil. *Environ Pollut*, (Barking, Essex: 1987) *212*, 230–237. <https://doi.org/10.1016/j.envpol.2016.01.069>
45. Yu, X., Takabe, Y., Yamamoto, K., Matsumura, C., & Nishimura, F. (2016). Biodegradation property of 8:2 fluorotelomer alcohol (8:2 FTOH) under aerobic/anoxic/anaerobic conditions. *J of Wat & Envir Tech*, *14*, 177–190. <https://doi.org/10.2965/jwet.15-056>
46. Bell, C. H., Gentile, M., Kalve, E., Ross, I., Horst, J., & Suthersan, S. (2019). *Emerging contaminants handbook*. CRC Press.
47. Schroll, R., Becher, H. H., Dörfler, U., Gayler, S., Grundmann, S., Hartmann, H. P., & Ruoss, J. (2006). Quantifying the effect of soil moisture on the aerobic microbial mineralization of selected

- pesticides in different soils. *Environmental Science and Technology*, 40, 3305–3312. <https://doi.org/10.1021/es052205j>
48. Tao, L., & Yang, H. (2011). Fluroxypyr biodegradation in soils by multiple factors. *Environmental Monitoring and Assessment*, 175, 227–238. <https://doi.org/10.1007/s10661-010-1508-2>
 49. Chandra, S., Sharma, R., Singh, K., & Sharma, A. (2013). Application of bioremediation technology in the environment contaminated with petroleum hydrocarbon. *Annales de Microbiologie*, 63, 417–431. <https://doi.org/10.1007/s13213-012-0543-3>
 50. Gassmann, M. (2021). Modelling the fate of pesticide transformation products from plot to catchment scale-state of knowledge and future challenges. *Front Environ Sci*, 9. <https://doi.org/10.3389/fenvs.2021.717738>
 51. Boesten, J. J. T. I., & Linden, A. M. A. (1991). Modeling the influence of sorption and transformation on pesticide leaching and persistence. *Journal of Environmental Quality*, 20, 425–435. <https://doi.org/10.2134/jeq1991.00472425002000020015x>

Publisher's Note Springer Nature remains neutral with regard to jurisdictional claims in published maps and institutional affiliations.